

M. PISAREK*, A. ROGUSKA*, L. MARCON**, M. ANDRZEJCZUK***, M. JANIK-CZACHOR*

ENHANCED BIOACTIVITY OF CALCIUM PHOSPHATE COATINGS OBTAINED BY A DIRECT ELECTRODEPOSITION FROM HANKS' SOLUTION ON Ti SURFACE

ZWIĘKSZONA BIOAKTYWNOŚĆ POWŁOK FOSFORANOWO-WAPNIOWYCH OTRZYMANÝCH METODĄ BEZPOŚREDNIEGO ELEKTROOSADZANIA NA POWIERZCHNI Ti Z ROZTWORU HANKA

The main requirements for titanium biomaterials are: (a) biocompatibility, (b) resistance to biological corrosion and (c) antisepticity. These requirements may be met by a new generation of titanium biomaterials with a specific surface layer of strictly defined microstructure, chemical and phase composition. Recently, various surface modifications have been applied to form a bioactive layer on Ti surface, which is known to accelerate osseointegration.

The purpose of this study was to investigate bioactivity of porous calcium phosphate coatings prepared by a direct electrodeposition on Ti surface from a modified Hanks' solution. The thick 200 nm coatings, were prepared via cathodic polarization at constant voltage -1.5 V vs. OCP in a Hanks' solution. In order to evaluate the potential use of the coatings for biomedical applications, the adsorption of bovine serum albumin (BSA), the most abundant protein in blood, and living cells attachment (osteoblasts, U2OS) were studied. The observed differences in living cells attachment suggest a more promising initial cellular response of Ca-P coatings with a pre-adsorbed albumin.

The topography and a cross-section view of the Ca-P coatings were characterized using SEM and STEM techniques. The surface analytical techniques (AES, XPS, and FTIR) were used to characterize their chemical composition before and after protein BSA adsorption.

Keywords: biocompatibility, Ca-P coatings, electrodeposition, BSA protein, osteoblasts (U2OS)

Wymagania stawiane biomateriałom tytanowym to przede wszystkim: (a) biozgodność, (b) odporność na korozję oraz (c) antyseptyczność. Wymagania te mogą zostać spełnione poprzez wytworzenie nowej generacji biomateriałów tytanowych o określonej powierzchni właściwej, z ściśle określoną mikrostrukturą, składem fazowym i chemicznym. Współcześnie znane są różne metody modyfikacji powierzchni Ti prowadzące do formowania bioaktywnych warstw, które przyspieszają proces osteointegracji.

Celem naszych badań było zbadanie bioaktywności porowatych powłok fosforanowo-wapniowych (Ca-P) przygotowanych poprzez bezpośrednie elektroosadzanie na powierzchni Ti z roztworu Hanka. Grubość wytworzonych powłok wynosiła około 200 nm, przy parametrach procesu elektroosadzania: napięcie – 1.5 V vs. OCP, czas 8000 s, roztwór Hanka. W celu dokonania oceny możliwości zastosowania badanych powłok dla potrzeb biomedycznych zastosowano adsorpcję albuminy surowicy bydlęcej (BSA), która jest najczęstszą występującą proteiną we krwi oraz testy komórkowe przyłączania się osteoblastów (linia komórkowa U2OS). Obserwowane zmiany podczas testów z żywymi komórkami sugerują bardziej obiecującą początkową odpowiedź dla powłok fosforanowo-wapniowych z wstępnie zaadsorbowaną albuminą.

Do obserwacji topografii powierzchni otrzymanych powłok oraz struktury na przekroju zastosowano mikroskopię wysoko- rozdzielczą SEM oraz TEM. Zastosowano również techniki powierzchniowo czułe: AES, XPS, FTIR w celu określenia składu chemicznego warstw przed oraz po adsorpcji protein na ich powierzchni.

1. Introduction

The development of biotechnology has resulted in a growing interest in interactions of proteins with organic and inorganic solids. In the recent years a special attention has been given to the studies of protein adsorption phenomena in solids. These studies have shown that adsorption of proteins on the surface of biomaterials contributes to improving their

biocompatibility (osseointegration) preceding the formation of biofilms [1]. Titanium is widely used for manufacturing of implants reconstruction. [2, 3]. This element has been regarded until recently as a biologically inert. However, recent clinical experience shows, that it may cause allergy or the inflammatory reaction at the bone-implant interface [3]. The way to improve the biocompatibility of titanium implants is electrochemical modification of their surfaces with bioactive phases

* INSTITUTE OF PHYSICAL CHEMISTRY, POLISH ACADEMY OF SCIENCES, KASPRZAKA 44/52, 01-224 WARSAW, POLAND

** FACULTY OF MATERIALS SCIENCE AND ENGINEERING, WARSAW UNIVERSITY OF TECHNOLOGY, WOŁOSKA 141, 02-507 WARSAW, POLAND

*** INTERDISCIPLINARY RESEARCH INSTITUTE, USR CNRS 3078 PARC DE LA HAUTE BORNE, 50 AV. DE HALLEY 59658 VILLENEUVE D'ASCQ, FRANCE

which improve osseointegration [4, 5]. The basic factors which significantly affect the biological processes occurring at the material-cell/tissue interface include (a) surface topography, (b) chemical and phase composition, and (c) physicochemical properties (e.g. wettability). In spite of intensive studies, no definitive criteria have yet been established which would describe topographic/morphological features of a biomaterial, optimal for the growth of particular types of cells. It is known, however, that titanium implants with a relatively highly developed surface show improved integration with bone tissue [6-8]. It has also been observed that a well-developed morphology and high porosity accelerate collagen synthesis and supports bone mineralization. The surface treatment of Ti has also a significant impact on adhesion and the rate of cell growth [9, 10]. It should be considered, however, that the given cells may react differently to the particular properties of an implant surface. The contact between a biomaterial and cells, tissues and body fluids results in the extra-cellular matrix proteins forming a biofilm on the surface. Cells attach themselves to this biofilm through integrin receptors and a specific sequence of extra-cellular matrix proteins. This influences their biological activity, including ability to proliferate and migrate [1, 11, 12]. The structure of the biofilm depends on the surface properties of the biomaterial, mainly on its chemical composition and morphology [13]. Thus, certain electrochemical processes have been employed for modifying surfaces of Ti in order to increase its biocompatibility [4, 5]. The chemical composition of the coatings obtained in this way is close to that of hydroxyapatite, one of the most effective materials for increasing biocompatibility.

In this work, cathodic polarization of Ti in Hanks' solution was used to form a bioactive calcium phosphate surface layer. The combined effects of surface topography and chemistry of the substrate on calcium phosphate formation were investigated. Moreover, to evaluate a potential use of the Ca-P/Ti coatings, thus obtained for biomedical implants, protein adsorption and living cells attachment on its surfaces were examined. Bovine serum albumin was used in this study to enhance biocompatibility of the Ca-P coatings while U2OS cells to test examining biological response.

2. Experimental

The substrate material was a 0.25 mm-thick Ti foils (99.5% purity, Alfa Aesar, USA). Samples 15 mm×15 mm square were ultrasonically cleaned with deionized (DI) water, rinsed with acetone and ethanol and dried in air. Calcium phosphate coatings were electrodeposited on the titanium from Hanks' solution. The solution was prepared by dissolving reagent-grade (g/L): NaCl 8.00, KCl 0.40, Na₂HPO₄·2H₂O 0.06, KH₂PO₄ 0.06, MgSO₄·7H₂O 0.20, NaHCO₃ 0.35, CaCl₂ 0.14 into distilled water and buffering at pH = 7.4. The electrodeposition of calcium phosphates was performed at room temperature at constant cathodic potential – 1.5 V vs. OCP potential (10 min.) for 8000 s in a conventional cell consisting of Ag/AgCl (3M KCl) reference electrode, the platinum counter electrode and working electrode (pure Ti). Titanium substrates were used as cathodes for electrodeposition. The cathodic polarization process was performed using an

AutoLab PGSTAT 302N (Ecochemie) potentiostat/galvanostat. After the electrodeposition, all samples were rinsed with DI water and dried in air.

The morphology of the electrodeposited coatings on Ti, top-view, and cross-sections were examined with a scanning electron microscope (Hitachi S-5500) and a scanning transmission electron microscope (Hitachi HD 2700). A Thermo Noran X-ray energy dispersive spectrometer coupled with SEM and STEM microscopes were used for local element analysis. A single focused ion beam (FIB) system Hitachi FB-2100 (Hitachi High Technologies Corporation, Japan) was used for specimen preparation for electron microscopic examinations.

Bovine serum albumin (BSA), (Sigma, purity of 99.8%) was a model protein in this study. Phosphate buffered saline (PBS, pH=7.4) was used to prepare the protein solution. 100 μ l of the protein solution (10 mg/ml protein/PBS) were pipetted onto the calcium phosphate coating in a cell culture plate. The plate was then placed in an incubator at 37°C for 20 min. The samples were examined immediately after termination of the preparation procedure.

The high resolution scanning Auger microprobe, MicroLab 350 (Thermo Electron) was applied in order to monitor the chemical composition and chemical states of the elements of the calcium phosphate coatings before and after adsorption of the proteins, utilizing the XPS function of the instrument with a lateral resolution of about several mm, and depth resolution ~10 nm.

Fourier transform infrared spectroscopy (FT-IR; Nicolet iN10-MX, Thermo Scientific) was used to examine phase composition and structural aspects of the calcium phosphate coatings after electrodeposition from Hanks' solution and after adsorption of proteins. The experiments were carried out using the reflectance mode and the MCT detector. The spectral resolution was equal to 4 cm⁻¹.

All samples were sterilized by autoclaving at 121°C for 20 min prior to cell culture experiments. Human osteosarcoma U2OS cells were used to evaluate the biocompatibility of the Ca-P coatings under study. Dulbecco's modified eagle's medium (DMEM, Invitrogen) supplemented with 10% fetal bovine serum (Invitrogen) and 1% of a penicillin/streptomycin mixture was used as a cell culture medium. Cells were seeded on the sample surfaces at 1.0×10⁴ cells/cm² and cultured at 37°C in a humidified atmosphere containing 5% CO₂ for 72 and 120h. Afterwards, double fluorescent labeling of the cell nuclei and membranes was performed. The cell nuclei were stained with Hoechst 33342 (Invitrogen), and the cell membranes were stained with Vybrant DiI (Molecular Probes) according to the manufacturers' instructions. The morphology of the cells was examined using a fluorescence microscope (Eclipse 80i, Nikon Instruments, Tempe, AZ).

3. Results and discussion

3.1. Morphology, structure

SEM images of a typical morphology of the Ti after electrodeposition process in Hanks' solution are shown in Fig. 1. The mechanism of cathodic electrodeposition of calcium phosphate layers from simulated body fluids (e.g. Hanks' solution)

on Ti surface has been discussed already in many scientific papers [14, 15]. In general, under the application of a DC voltage, the following reaction occurs on the cathode:

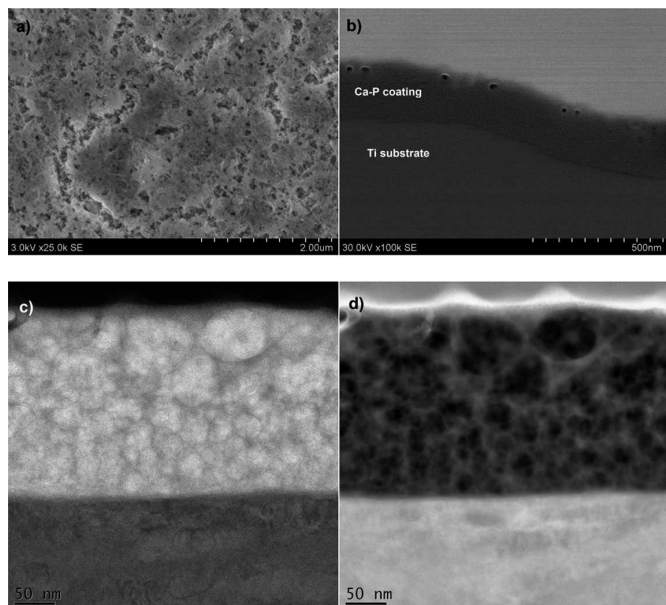
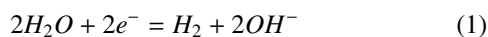


Fig. 1. SEM images of the electrodeposited Ca-P coating: top-view (a), cross sections view (b), STEM images of the Ca-P cross sections presented in various modes of microscope operation: BF-STEM (c), Z-contrast (d)



This reaction increases the pH value in the vicinity of the cathode surface and hence increases the supersaturation corresponding to Ca-P. The Ca^{2+} ions migrate to the cathodic Ti substrate to react with the PO_4^{3-} and OH^- ions there to form a calcium phosphates layer on the surface. The bath temperature, the voltage, and the current density affect the composition and crystal structure of the coatings [14-16]. The details of the mechanism of the formation of such layers can be found in the publications [14, 15].

SEM examinations revealed that the calcium phosphate coatings exhibit a developed porous morphology characterized by a network of longitudinal pores of different shapes (Fig. 1a). Fig. 1b shows a cross-sectional view of the Ca-P layer obtained using the SEM technique. The thickness of the cathodic electrodeposited layer after polarization process is about 200 nm (Fig. 1b). The SEM images of the Ca-P coatings suggest that electrodeposition from Hanks' solution at the potential -1.5V vs OCP leads to formation of a morphologically quite homogenous layer with a good adhesion to the substrate (Fig. 1 c, d). The STEM images taken under higher magnification (Fig. 1c, d) show a subtle porosity of the Ca-P layer. Well visible nanopores are uniformly distributed across the "sponge like structure" with a decrease of the pore size with depth. Larger pore size within the upper part of the porous layer may assure better integration with bone. The obtained morphology, structure are similar to that reported in the literature [4, 17], and seem to be promising for biomedical applications.

3.2. Chemical and phase composition of the Ca-P coatings

Before adsorption of the proteins and attachment of the living cells on the surface of the Ca-P coatings, all the samples were subjected to a sterilization process in autoclave [18]. Such sterilization is widely used in production of biomedical devices. Thus, it was important to check whether or not it results in a change of the chemical composition of the coatings. The EDS results showed that, in fact, it leads to an enrichment of the layer with Ca and P. The average concentration of Ca and P does not drastically change after sterilization treatment. The atomic concentration ratio Ca/P for as-coated samples is about 1.38 and about 1.27 for autoclaved ones (see Table 1). The results presented in Table 1 show also that Ca/P atomic ratio for both coatings vary from place to place, which suggests that electrodeposition process is not fully homogenous, so there are local differences in chemical composition. Local supersaturation and pH fluctuations during electrodeposition may cause formation of metastable transient Ca-P phases like DCP, OCP, ACP(Ca/P = 1.0-2.2) [19]. The composition of the coating – as the EDS analysis and the estimated average molar Ca/P ratio suggest – may correspond to octacalciumphosphate (OCP, Ca/P = 1.33) and probably to various intermediate Ca-P phases [20, 21]. The OCP compound is known as a precursor for the crystallization of bone-like apatite/hydroxyapatite [19].

TABLE 1
Results of local EDS analysis (Ca/P ratio) of calcium phosphate coatings electrodeposited on Ti from Hanks' solution

EDS results	Ca/P at.% local ratio	Ca/P at.% ratio, average value
Ti/Ca-P -1.5 V vs. OCP	1.17-1.64	1.38
Ti/Ca-P -1.5 V vs. OCP after sterilization in autoclave, temp.121°C	1.03-1.36	1.27

In order to evaluate the chemical state of the calcium and phosphorous in the uppermost part of the coatings electrodeposited on titanium, XPS measurements were performed. This technique provides an average information from a geometrical surface area of about 2 mm×5 mm. The chemical state can be evaluated on the basis of the thus determined Ca/P molar ratio, as already reported earlier [8]. Table 2 shows the binding energies of the O 1s, Ca 2p_{3/2}, and P 2p_{3/2} signals, and the suggested chemical composition. The main peak of P 2p_{3/2} may change within the range of 132.8-133.4 eV for electrodeposited coatings. The spectral data for Ca suggest also the presence of calcium phosphate compounds (Ca 2p_{3/2}: 347.5-347.9 eV) [8, 20, 22-25]. The main component of the O 1s peak at BE = 531.4-531.6 eV is attributed to PO_4^{3-} groups [8, 20, 22-25]. The results suggest that a calcium phosphate layer apatite-like is formed on Ti substrate, see Table 2, and compare also discussion in Ref [8].

X-ray photoelectron spectroscopy analysis confirmed that the surface is enriched with calcium (Ca) and phosphorous (P), with a Ca/P molar ratio of 1.10. However, the XPS measurements provide surface information from a few uppermost

TABLE 2

Ca 2p_{3/2}, P 2p_{3/2} and O 1s binding energies for an electrodeposited coatings from Hanks' solution as measured from the corrected XPS spectra. Surface compounds were evaluated using a deconvolution procedure to estimate Ca/P ratio (data taken and calculated for 8 samples)

Ti/Ca-P -1.5 V vs. OCP	Ca2p _{3/2} / eV	P2p _{3/2} eV	O1s/eV	chemical state	Ca/P at.% ratio, average value
after electrodeposition	347.5-347.9 /Ca ²⁺	132.8-133.4 /PO ₄ ³⁻	531.4-531.6	calcium- phosphates	1.10 (1.02-1.13)

nanometers of the samples [26]. Thus, XPS results suggest that during electrodeposition of the Ca-P coatings a different kind of Ca-P was formed than that suggested by EDS results. However, this phase is limited to the outermost part of the surface layer only. Careful inspection of the chemical composition near the uppermost layer revealed that, Ca/P molar ratio changed within the Ca-P coating depth. Fig. 2 presents a partial compositional profile (the relative Ca/P atomic molar ratio) of the electrodeposited layer on Ti, as measured with XPS combined with ion sputtering. As seen from Fig. 2, Ca/P concentration ratio is distinctly higher within the layer than at the surface. After 300 s of etching (which corresponds to a thickness about 12 nm, based on a sputtering rate 0.04 nm/s) the Ca/P atomic molar ratio is close to 1.43. This finding correlates with the results of EDS measurements (1.38, see Table 1). After 600 s of sputtering the Ca/P atomic ratio remains on the same level, apparently the chemical composition does not change further with depth. The difference in the molar Ca/P ratio between the bulk and the outermost layer of the coating is evidently significant. This shows that the very thin outermost part of the layer apparently a compact one, has a different chemical composition (apparently a compact one) than the bulk of it, which is highly porous (compare Fig. 1c and 1d).

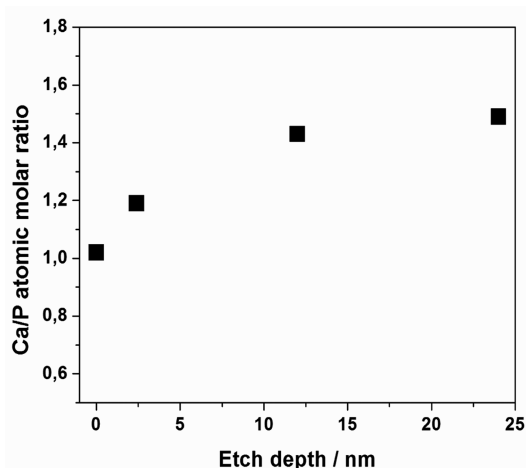


Fig. 2. Typical Ca/P atomic molar ratio vs. sputtering depth for electrodeposited coatings on Ti

Fourier transform infrared (FTIR) spectroscopy was used to obtain additional information on the chemical composition of the Ca-P coatings before and after sterilization process. Hydroxyapatite, the main mineral component of biological bone, with its formula of Ca₁₀(PO₄)₆(OH)₂, absorbs IR radiation due to the vibrational modes from the phosphate and hydroxyl groups. In biological apatite (type B), some PO₄³⁻ ions are substituted by CO₃²⁻ ions, and the IR technique is

very sensitive to such carbonate substitutions, so even a small amount of carbonate can be detected [27]. FTIR spectra of the calcium phosphate coating electrodeposited on Ti are shown in Fig. 3. These spectra are dominated by the main PO₄³⁻ vibration mode. The bands detected at 1490, 1420 and 870 cm⁻¹ were assigned to the carbonates group (CO₃²⁻). Well-defined band at 870 cm⁻¹ in the spectra may suggest that some PO₄³⁻ ions are substituted by CO₃²⁻ ions. Such substitution is characteristic of B-type carbonated apatite. However, the peak at 870 may also suggest the presence of HPO₄²⁻, as well [28, 29]. Hence a final conclusion requires a more detailed analysis of C1s XPS peak, as discussed below.

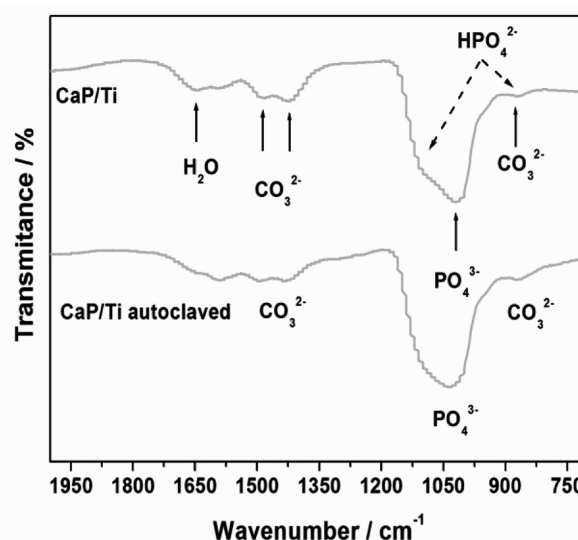


Fig. 3. FTIR spectra of Ca-P layer before and after sterilization process in autoclave

The detailed studies of the XPS carbon peak at different times of the ion etching revealed carbonate groups at the surface of the Ca-P layer. The high-resolution XPS spectrum of C1s (Fig. 4) shows a main peak at 285.0 eV due to carbon bonds from the surface contamination and components at higher binding energies which correspond to various chemical bonding of carbon with oxygen. The C1s high-resolution XPS spectrum indicates clearly the presence of carbonate group at 290.7 eV [23], which is in agreement with the findings of FTIR investigation. The presented results FTIR and XPS suggest that during electrodeposition of Ca-P layer carbonate apatite is formed, which is similar to the bone apatite.

The above reported results suggest that the electrodeposited Ca-P coatings on Ti may be promising substrate for protein adsorption and living cells attachment. Subtle differences in the chemistry of the surface of Ca-P coatings may result in significant differences in cell behavior. Therefore, such layer has

attracted the attention of materials scientists and biochemists recently.

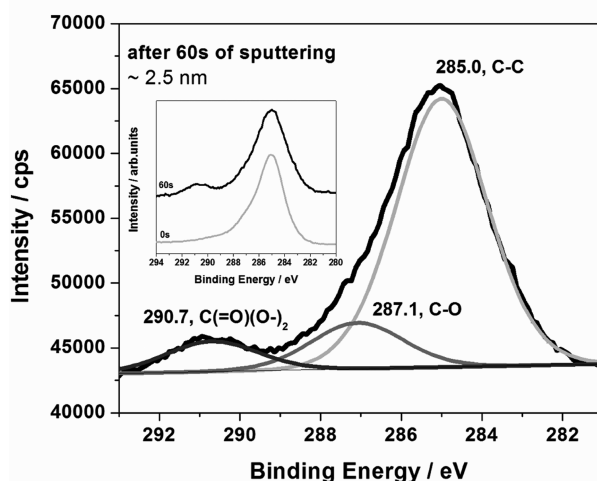


Fig. 4. High-resolution XPS spectrum of C1s peak after 60s of sputtering of Ca-P electrodeposited coating. Insert shows high resolution XPS spectra of carbon before and after sputtering process

3.3. Adsorption of proteins (BSA)

Table 3 presents the binding energies of the C1s, N1s, Ca2p_{3/2} and P2p_{3/2} signals and the suggested chemical state of the surface components for Ca-P samples investigated after protein adsorption. The XPS reference data for pure albumin is also given. The N1s high-resolution XPS spectrum indicates clearly the presence of N-C=O, C-N, and N-H characteristics protein functional groups at ~400.0, ~398.5 and ~402.0 eV, respectively [1, 8, 10, 22]. The carbon species expected from the bases included the main hydrocarbon (C-H: 285.0 eV), carbon bounded to nitrogen (C-N: ~286.5), amide carbon (N-C=O: ~288.0 eV) and carbon bounded to oxygen (C=O: ~290.0 eV) [1, 8, 10, 22]. Moreover, the signals of Ca and

P are also present, apparently evolving from the components of the electrochemically deposited layer. This suggests that the protein molecules are adsorbed on the calcium phosphate coatings before and after sterilization process in autoclave.

FTIR measurements of the BSA adsorbed on the surfaces under investigation coincide with the XPS results. Plasma protein was found to be adsorbed on the surfaces under investigation. FTIR spectrum of BSA adsorbed on electrodeposited coating is presented in Fig. 5. The band at ~1655 have been assigned for amides I [30, 31]. The band due to amide II is not observed for Ca-P layer, as compared to the reference BSA sample, where it appears at 1535 cm⁻¹. This may be a result of some changes in the protein tertiary structure (3D) due to the interactions with the surfaces investigated. The chemistry and morphology of the substrate may play a role here. Probably initial cellular response to the Ca-P surface is expected to be different because of the differences in the state of adsorbed protein, as compared to the protein not adsorbed (reference), see Fig. 5.

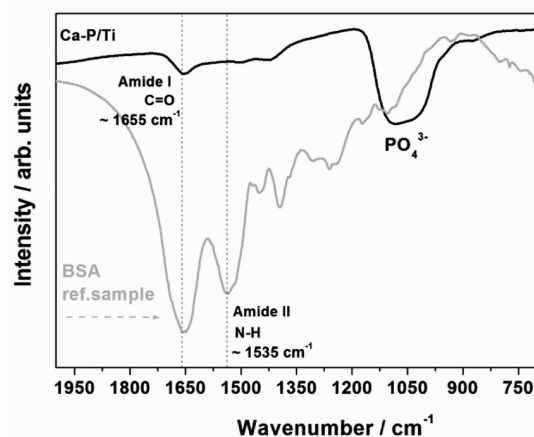


Fig. 5. FTIR spectrum of BSA proteins adsorbed on the electrodeposited Ca-P layer, reference spectrum of BSA is also given

TABLE 3

C1s, N1s, Ca2p_{3/2} and P2p_{3/2} binding energies as measured with XPS and suggested surface chemical species for samples after protein adsorption

Samples	Ca2p _{3/2} /eV	P2p _{3/2} eV	C1s eV	N1s eV	chemical state
Ti/Ca-P -1.5 V vs. OCP	347.2	132.8	288.1 286.5 285.0 289.9	400.2 398.5 402.1	Ca ²⁺ , PO ₄ ³⁻ N-C=O C-N N-H C-C/C-H C=O
Ti/Ca-P -1.5 V vs. OCP after sterilization in autoclave, temp.121°C	347.5	133.0	288.1 286.4 285.0 289.9	400.1 398.3 402.1	Ca ²⁺ , PO ₄ ³⁻ N-C=O C-N N-H C-C/C-H C=O
pure albumin/ ref. sample			288.2 286.6 285.0 290.0	400.2 398.6 402.1	N-C=O C-N N-H C-C/C-H C=O

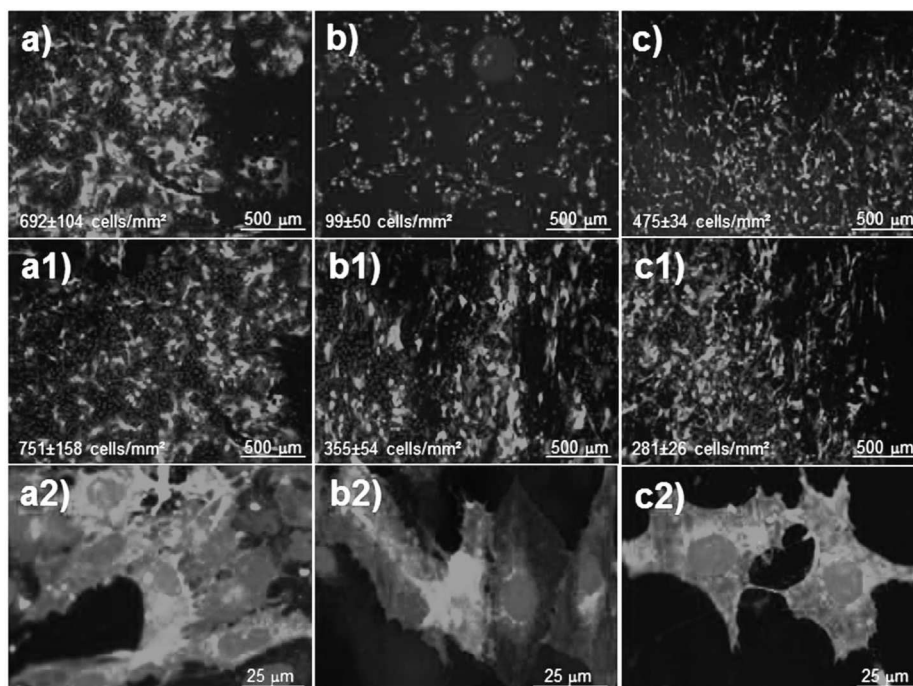


Fig. 6. Fluorescence microscopy images of U2OS cells cultivated for 72 h (a, b, c) and 120 h (a1, b1, c1, a2, b2, c2) on the electrodeposited Ca-P coatings on Ti without and with BSA proteins. Cell density was calculated by averaging 6 images taken randomly from the same surface: a) reference sample, culture dish, b) Ti/Ca-P: -1.5 V vs. OCP after sterilization in autoclave, c) Ti/Ca-P: -1.5 V vs. OCP after sterilization in autoclave + BSA proteins

3.4. Cell culture experiments

Data reported [32, 33] in the literature suggested that BSA may exhibit a specific binding interaction with apatite/hydroxyapatite which may result in an improvement of the osteoblast cells adhesion and proliferation. These findings, taken in a relation to present results, suggest that it might be possible to develop a better Ca-P-based biomaterial through an incorporation of albumin into the mineral matrix to improve its capacity for cell adhesion and proliferation [32, 33].

Our preliminary results of the response of human osteosarcoma U2OS cells to the surfaces investigated are in qualitative agreement with the protein adsorption measurements. Fig. 6 shows the cells on the Ti with electrodeposited Ca-P coatings before and after adsorption of BSA proteins. Fluorescence microscopy observations revealed that the amount of U2OS cells after 72 h incubation is distinctly higher on the Ca-P coating with adsorbed albumin than for the sample without proteins (compare Fig. 6 b and c). A series of investigations by Yamaguchi and coworkers [33, 34] have suggested that albumin is released by the osteoblast cells adhered to the fracture healing sites and this excess albumin increases proliferation of the surrounding cells. In our study, the surface modification with BSA led to significant improvement in osteoblast-like cells binding to an electrodeposited Ca-P coating. Similar observation, but for MC3T3-E1 cells were reported by other authors [32-34], who have found that adsorption of BSA to the surface of conventional and nanophase ceramic (including hydroxyapatite) influences the proliferation/differentiation of adherent cells. After 120 h of incubation, however, the increase in cell number is observed only for surface without BSA (see, Fig. 6 b1, c1). Such a result could

be expected. Usually a longer time of incubation increase proliferation of the living cells. Probably, the adsorption of BSA affects positively the kinetics of proliferation of the attached cells and so the process of proliferation terminates earlier in the such case.

Our fluorescence microscopy observations for both coatings at higher magnifications revealed that the cells are well extended and exhibit an elongated morphology, similar to those on the reference sample (culture dish, Fig. 6 a2). The nuclei are clearly shaped, but the cell membranes form a dendritic structure. After 120 h of incubation the cells on both coatings (with and without albumin) exhibited cytoplasmic links, as shown in Fig. 6 b2, c2. After this time, the cells were well attached on the surface of the electrodeposited Ca-P coating with an extending cytoplasmic process [5, 35, 36].

4. Conclusions

The present investigations shows that calcium phosphate coatings of porous apatite-like structure and a specific morphology can be grown by electrodeposition at -1.5 V vs. OCP in the Hanks' solution on pure titanium. A porous Ca-P layer with a pore size gradient with an apparently compact thin overlayer is formed. Our EDS and XPS results suggest that carbonated apatite may be formed during electrodeposition process. The results of XPS and FTIR investigations imply that bovine serum albumin (BSA) adsorbed readily on such calcium phosphate coating. The Ca-P surface with pre-adsorbed protein enhances cell attachment, which leads to achieving biocompatibility faster. Thus, one may anticipate that electrodeposited Ca-P coating on Ti may promote early bone apposition and

implant fixation by enhancing the chemical bonding between new bone and the surface of implant materials.

Acknowledgements

This work was financially supported by the Polish Ministry of Science and Higher Education (Grand no. N N507 355035), the National Science Center (decision No. DEC-2011/01/B/ST5/06257) and by the Institute of Physical Chemistry PAS (Warsaw, Poland) and Interdisciplinary Research Institute (Lille, France).

REFERENCES

- [1] K. Cai, J. Bossert, K.D. Jandt, *Colloids and Surf. B: Biointerfaces*. **49**, 136 (2006).
- [2] H.J. Rack, J.I. Qazai, *Mat. Sci. Eng. C*. **26**, 1269 (2006).
- [3] D.M. Brunette, P. Tengvall, M. Textor, P. Thomsen, *Titanium in Medicine: Material Science, Surface Science, Engineering, Biological Responses and Medical Applications (Engineering Materials)*, Springer-Verlag Berlin Heidelberg, 2001.
- [4] Ji-H. Park, D.-Y. Lee, K.-T. Oh, Y.-K. Lee, K.-M. Kim, K.-N. Kim, *Mat. Let.* **60**, 2573 (2006).
- [5] J.H. Park, Y.-K. Lee, K.-M. Kim, K.-N. Kim, *Key Eng. Mat.* **284-286** 473 (2005). Trans Tech Publications, Switzerland.
- [6] X. Liu, P.K. Chu, Ch. Ding, *Mat. Sci. Eng. R*. **47**, 49 (2004).
- [7] M. Lewandowska, A. Roguska, M. Pisarek, B. Polak, M. Janik-Czachor, K.J. Kurzydłowski, *Biomole. Eng.* **24**, 438 (2007).
- [8] M. Pisarek, A. Roguska, M. Andrzejczuk, L. Marcon, S. Szunerits, M. Lewandowska, M. Janik-Czachor, *Appl. Surf. Sci.* **257**, 8196 (2011).
- [9] J. Wang, P. Layrolle, M. Stigter, K. de Groot, *Biomaterials*. **25**, 583 (2004).
- [10] D.D. Deligianni, N. Katsala, S. Lada, D. Sotiropoulou, J. Amedee, Y.F. Missirlis, *Biomaterials*. **22**, 1241 (2001).
- [11] K. Cai, M. Frant, J. Bossert, G. Hildebrand, K. Liefelth, K.D. Jandt, *Colloids Surf. B: Biointerfaces*. **50**, 1 (2006).
- [12] X. Zhu, J. Chen, L. Scheideler, R. Reichl, J. Geis-Gerstorfer, *Biomaterials*. **25**, 4087 (2004).
- [13] B. Feng, J. Weng, B.C. Yang, S.X. Qu, X.D. Zhang, *Biomaterials*. **24**, 4663 (2003).
- [14] M.S. Djosic, V. Panic, J. Stojanovic, M. Mitric, V.B. Miskovic-Stankovic, *Colloids and Surfaces A: Physicochem. Eng. Aspects*. **400**, 36 (2012).
- [15] A. Rakngarm, Y. Mutoh, *Mater. Sci. Eng. C*. **29**, 275 (2009).
- [16] M.V. Popa, J.M. Calderon Moreno, M. Popa, E. Vasilescu, P. Drob, C. Vasilescu, S.I. Drob, *Surf. Coat. Technol.* **205**, 4776 (2011).
- [17] H. Wang, N. Eliaz, L.W. Hobbs, *Mat. Let.* **65**, 2455 (2011).
- [18] S.V. Dorozhkin, M. Schmitt, J.M. Bouler, G. Daculsi, *J. Mat. Sci. Materials in Medicine*. **11**, 779 (2000).
- [19] S.V. Dorozhkin, *J. Mat. Sci.* **42**, 1061 (2007).
- [20] H.B. Lu, C.T. Campbell, D.J. Graham, B.D. Ratner, *Anal. Chem.* **72**, 2886 (2000).
- [21] M. Vallet-Regi, J.M. Gonzalez-Calbet, *Progress in Solid State Chem.* **32**, 1 (2004).
- [22] A. Roguska, M. Pisarek, M. Andrzejczuk, M. Dolata, M. Lewandowska, M. Janik-Czachor, *Mat. Sci. Eng. C*. **31**, 906 (2011).
- [23] J. Chastain, R.C. King Jr. (Eds.), *Handbook of X-Ray Photoelectron Spectroscopy, A Reference Book of Standard Spectra for Identification and Interpretation of XPS Data*, Physical Electronics, Inc., USA 1995.
- [24] P. Royer, Ch. Rey, *Surf. Coat. Technol.* **45(1-3)**, 171 (1991).
- [25] T. Hanawa, M. Ota, *Biomaterials*. **12(8)**, 767 (1991).
- [26] J.W. Niemantsverdriet, *Spectroscopy in catalysis*, Wiley-VCH VerlagGmbH&Co. KGaA, Weinheim, 39 (2007).
- [27] A. Stoch, W. Jastrzębski, A. Brożek, B. Trybalska, M. Cichocińska, E. Szarawara, *J. Molecular Structure*. **511-512**, 287 (1999).
- [28] L. Muller, E. Conforto, D. Caillard, F.A. Muller, *Biomolecular Eng.* **24**, 462 (2007).
- [29] C. Rey, C. Combes, C. Drouet, H. Sfihi, A. Barroug, *Mat. Sci. Eng. C*. **27**, 198 (2007).
- [30] H. Zeng, K.K. Chittur, W.R. Lacefield, *Biomaterials*. **20**, 377 (1999).
- [31] J. Twardowski, P. Anzenbacher, *Raman and IR spectroscopy in biology and biochemistry*, Polish Scientific Publishers PWN Ltd., Warsaw, 1994.
- [32] M.T. Bernards, C. Qin, S. Jiang, *Colloids Surf. B: Biointerfaces*. **64**, 236 (2008).
- [33] M. Yamaguchi, A. Igarashi, H. Misawa, Y. Tsurusaki, *J. Cellular Biochem.* **89(2)**, 356 (2003).
- [34] K. Ishida, M. Yamaguchi, *Inter. J. Molecular Medicine*. **14(6)**, 1077 (2004).
- [35] P.J. ter Brugge, S. Dieudonne, J.A. Jansen, *J. Biomed. Mat. Res. A*. **61(3)**, 399 (2002).
- [36] X. Zhu, J. Chen, L. Scheideler, R. Reichl, J. Geis-Gerstorfer, *Biomaterials*. **25**, 4087 (2004).

Received: 10 February 2012.